Small scale Cluster observations of current sheet disruptions during substorm

0. Le Contel, F. Sahraoui, A. Roux, D. Fontaine, P. Robert, J.-A. Sauvaud, C. Owen, and A. Fazakerley

Abstract: We present a substorm event and show that the pre-existing thin current sheet with a thickness of the order of the proton Larmor radius and current carried by electron (in the spacecraft frame) thickens under the effect of electromagnetic fluctuations at three scales: (1) low-frequency drift waves ($\simeq$ 20 mHz), (2) proton cyclotron / electron bounce waves ($0.2 - 10$ Hz), (3) whistler waves ($40 - 180$ Hz)). We focus on the latter type and show that they are associated with small scale current structure ($c/\omega_{pe} < l < c/\omega_{pi} \simeq \rho_i$).

Key words: current sheet thickening, proton cyclotron/ electron bounce resonance, whistler waves.

1. Introduction

Schematically two categories of substorm models can be distinguished depending on the onset location [19] : (i) the near-earth neutral line models where an X-line at $X \sim -23R_E$ produces earthward and tailward flows; the pileup of these earthward flows accounting for the tailward propagating front of the dipolarization. (ii) current disruption models where a micro-instability interrupts the cross-tail current which is diverted toward the ionosphere first between $6 - 15R_E$.

Analytically, these two categories are also clearly distinct [30]. The formation of a near-earth neutral line is understood as resulting from a tearing instability characterized by a wave vector $k_x \gg k_y$ along the magnetotail therefore perpendicular to the equilibrium cross-tail current J_y (e.g. [38]). On the other hand, the current disruption models rely upon instabilities with a wave vector $k_y \gg k_x$ along the cross-tail current and producing parallel and perpendicular current signatures modulated in the y direction.

These two categories of models have induced two types of data analysis. Indeed in the former case the time-variation of the magnetic field are interpreted as a signature of a steady structure, the so-called "Hall current system" with its characterized quadrupolar By signatures (e.g. [32]), moving across the spacecraft (s/c) whereas in the latter case magnetic structures are interpreted as signatures of azimuthally moving unstable waves passing by the s/c (e.g. [31, 6]).

The mechanism of energy dissipation characterized by its temporal and spatial scales can be considered as a way to distinguish between these different models. Indeed in a weakly collisional or collisionless plasma, the identification of the processes which lead to the energy dissipation is a longstanding issue. Again in the former class, often called collisionless magnetic reconnection models, it is suggested that the energy dissipation occurs at different scales for ions and electrons. It is shown that ions are decoupled from the magnetic field by Hall terms (in the generalized Ohms law) at a scale corresponding to their inertial length c/ω_{pi}. This scale being larger than the electron scale, the reconnection rate is found to increase compared with classical resistive MHD rate, where ions and electrons are not considered separately. In the region in between ion and electron inertial lengths, the electrons are still magnetized whereas ion dynamics can be neglected; the dynamics is expected to be controlled by whistler waves (e.g. [22, 4]). In the latter class, the energy dissipation can occur at many scales from the largest corresponding to the scale of the length of the magnetic field line via field line or bounce resonance(e.g. [39]) to the smallest via the ion and electron Larmor radius scales (e.g. [8, 9]). All these processes can be present simultaneously. The present data analysis belongs to the latter category. We present a substorm event observed by Cluster and interpret the observations as a tailward propagating thickening of the current sheet as described by [24] resulting from different kind of unstable waves at different scales.

Received 24 May 2005.

0. Le Contel, F. Sahraoui, A. Roux, D. Fontaine, and P. Robert. Centre d'étude des Environnements Terrestre et Planétaires (CETP), 10-12, avenue de l'Europe, F-78140 Vélizy, France.
J.-A. Sauvaud. Centre d'Etude Spatial des Rayonnements (CESR), 9 avenue du colonel Roche, F-31028 Toulouse cedex 4, France.
C. Owen and A. Fazakerley. Mullard Space Science Laboratory (MSSL), University College London, Dorking RH5 6NT, United Kingdom.

2. Observations

2.1. Global view

During the summer 2003, the average Cluster inter-satellite distance was about 200 km. Such a small distance allows accurate computations of the current density using the curlometer technique (e.g. [29]) even for very thin current sheets or relatively long wavelength waves ($\lambda > 200$ km) . We investigate a substorm event observed on August 17th 2003. Around 1650 UT Cluster was located at [-16.8,-5.55,3.33] R_E GSM. Most instruments were in burst mode. Magnetic field data are provided by the FGM instrument at 14.87 ms time resolution [3]. Ion and electron particles data come from CIS [28] (only CODIF on C4 is available) and PEACE [14] respectively. The time resolution for the moment calculation is 4 s for both particles instruments but the burst mode allows us to display electron spectrograms with time resolution of 125 ms. High- frequency fluctuations of magnetic and electric fields are provided by STAFF [7] and EFW [11] instruments. Their time resolution is 2.22 ms (450 sample/s). Data from different satellite

are displayed using the following color code: black for C1, red for C2, green for C3 and blue for C4. According to the

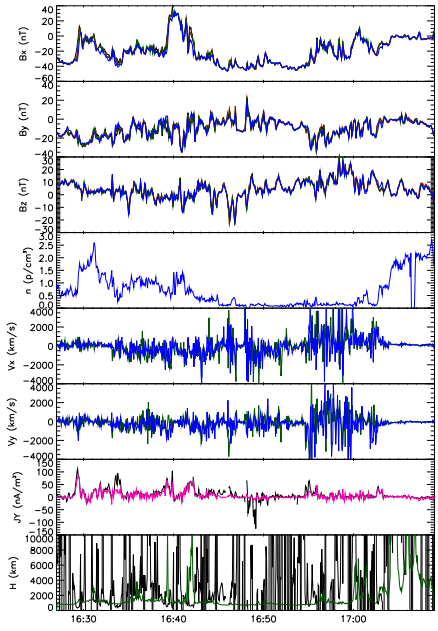

Fig. 1. All data are plotted in GSM coordinates: B_x, B_y, B_z components of the magnetic field, ion density, V_x and V_y components of the electron (thin line) and ion (thick line) velocities, J_y component of the electrical current density computed from curlB (pink line) and equatorial value of the J_y current density estimated from a Harris model (black line), half-thickness of the current sheet estimated from a Harris model (see text for details).

Kyoto quick look AE monitor (not shown), the magnetic activity was high as the AE reaches 1000 nT around 1700 UT indicating that we are probably observing a large substorm. Fig. 1, first panel, shows that from 1627 UT to 1709 UT, while the spacecraft cross the magnetic equator several times, the current sheet thickens as the GSM B_x component of the magnetic field varies from -40 nT to 0 nT. During this thickening three-dimensional electromagnetic waves are present at low-frequencies ($\simeq$ 20 mHz) as shown by the first three panels. The study of the low-frequency waves corresponding to the range of the so-called ballooning mode is out of the scope of the present paper but is carried out by [18]. On panel 4 the ion density profile corresponds to the expected variations as the s/c move from the central plasma sheet ($n_i \simeq 1.5$ p·cm^{-3}) to the boundary ($n_i < 0.1$ p·cm^{-3}). The V_x component of the electron velocity is larger than that of ions but shows the same variations from tailward, at the beginning of the interval, to earthward at the end (panel 5).The V_y component of the electron velocity is also larger than that of ions but is almost always dawnward (negative) whereas ion V_y is duskward (positive) except at the end of the interval where the electron and ion V_y have large positive as well as negative values (panel 6). On panel 7 the J_y current density computed using the curlometer technique (pink) is displayed as well as an estimate of the equatorial current density (black) from a Harris sheet model [12]. In order to compute the Harris current density we fitted the Bx component of the magnetic field measured by C1 and C3 with an instantaneous Harris sheet model defined by $Bx(t) = B_L(t)tanh((z(t) - z_0(t))/H(t))$ where z_0 and H represent the centre and the half-thickness of the current sheet, respectively. B_L is obtained either from direct measurements in the lobe region (if the s/c happen to be located in the lobes) or by assuming the equilibrium of the vertical pressure within the plasma sheet. Both computations lead to similar results during the interval.We find that Jy can increase up to 80 nA/m^2 and corresponds to the current carried by electron in the s/c frame ($J_{y,e} = -en_0V_{y,e} \simeq -e * 0.5$(p·cm $^{-3}$) * (-1000 (km/s)) $\simeq$ 75 nA/m^2) The fit with a Harris sheet has also been used to estimate the half-thickness of the CS (H) displayed on the last panel of Fig. 1. As soon as the s/c are located inside the CS, the fit works and gives a half-thickness which is around 1000 km or less. The green curve corresponds to the local ion Larmor radius computed at the location of C3. At the beginning of the interval, when all s/c are located far from the equator ($B_x \simeq -40$ nT) it corresponds to the ion Larmor radius computed in the asymptotic magnetic field of the Harris sheet model. During this period $H \simeq \rho_i$ (as well as c/ω_{pi}) and the observed CS structure agrees with the CS equilibrium models described by [34] in such a regime. Thus Cluster is observing a thin current sheet with large amplitude low-frequency electromagnetic fluctuations. The ion dynamics is very likely stochastic and the current is carried by electrons (in s/c frame see also [1]).

2.2. Ion scale observations

Now, we focus on a smaller time period (1659-1701 UT) corresponding to a fast thickening of the CS and a variation of B_x from - 30 nT to - 10 nT (Fig. 2). However, one should remark that even for these two-minutes time interval, the four s/c measure almost the same magnetic field, indicating that the spatial scale of the current sheet is larger than the average inter-satellite distance (200 km). Indeed for this time interval the estimated half-thickness from a Harris model is greater than 1000 km. Thus, the spatial scale of the CS is of the same order or larger than the proton Larmor radius, computed at the edge of the CS. However, the validity of the calculation of ion velocity in such a thin current sheet has been questionned by [41]. Between 1659:40 and 1700 UT, we observe a strong decrease of $|B_x|$ associated with large electric field fluctuations as well as quasi-dc electric field around 20 mV/m, and a large increase of the V_x component of the ion velocity (up to 1000 km/s), while the ion density remains constant. The same observations are obtained for electrons velocities up to 4000 km/s for C4 and to 3000 km/s for C3 (not shown) which confirms the ion moment calculation. Simultaneously, the current density obtained from curlB displays large amplitude oscillations on $J_x \simeq \pm$20nA/m^2 as well as on $J_y \simeq$ from $\pm$10 to $\pm$30 nA/m^2. Thus, ion acceleration seems to be associated with large amplitude current density fluctuations. One can remark that these correlations were also observed just a few seconds before and after, when all s/c were located at the edge of the current sheet (1659:10 UT- 165925 UT and 1700:10-1700:25 UT)), although with smaller amplitudes of the electric and magnetic fields and current density fluctuations. In order to better characterize the current density fluctuations we have

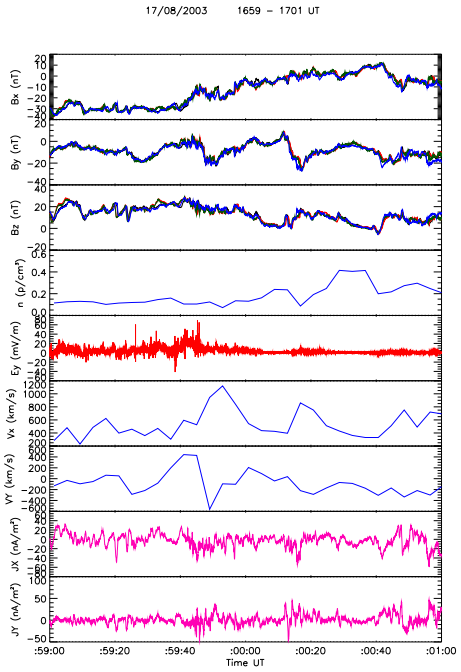

Fig. 2. All data are plotted in GSM coordinates excepted the electric field in SR2 frame: B_x, B_y, B_z components of the magnetic field, ion density, E_y component of the electric field, V_x and V_y components of ion velocity, J_x and J_y components of the electrical current density computed from curlB.

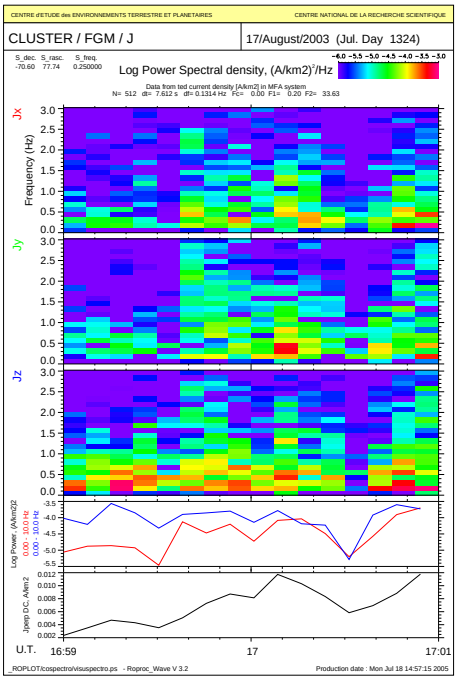

Fig. 3. Spectrograms of current density fluctuations computed from FGM data in a magnetic field aligned frame (J_z corresponding to $J_{\|}$). The time resolution of the spectrogram is 7.612 s and the frequency resolution is 0.1314 Hz. The lower cut-off frequency has been fixed at 0.2 Hz to be consistent with the magnetic field aligned frame mapping.

performed a spectrogram of the current density waveform obtained from FGM data, via the curlometer technique. Fig. 3 displays the three components of current density fluctuations in the (4 s average) magnetic field aligned (MFA) frame. The largest amplitude is found to correspond to the current density parallel to **B** (J_z) while the largest amplitude of the average magnetic field fluctuations is found to be in the perpendicular direction (not shown). Frequency range of these fluctuations corresponds to the proton cyclotron frequency ($f_{ci} \simeq 0.2-0.4$ Hz for $B_0 \simeq 15-30$ nT) as well as the electron bounce frequency $f_{be} \simeq v_e/L \simeq 0.15$ Hz for L = 20 R_E and $E_e = 1$ keV). We obtain the same results using the current density waveform computed from STAFF-SC data (not shown). These spectrograms show a clear signature of parallel current density fluctuations associated with a fast thickening of the CS which suggests a micro-instability as a source of these fluctuations, and that this instability is involved in this magnetic field reconfiguration.

2.3. Electron scale observations

Data gathering in burst mode on STAFF-SC allows us to analyse the magnetic wave form up to 180 Hz. Fig. 4 (left panel) displays the average Fourier spectrum computed from the sum of all 4.55 s duration (2048 points at 450 s/s) Fourier spectrum performed from 1627 to 1709 UT. Data have been moved in a (4 s average) MFA frame. We find that the spectrum is isotropic below 40 Hz and strongly anisotropic $\delta B_R \gg \delta B_{\|}, \delta B_L$ (R in red and L in green meaning classical right and left hand components when $\mathbf{k} \cdot \mathbf{B} > 0$) from 40 Hz to 180 Hz. Looking at the spectrogram on Fig. 4 (right panel) for the same time period, we observe that the anisotropic part of the spectra is caused by very intense short lasting emissions in the range below the electron cyclotron frequency, observed during the whole period. A wave polarization analysis, assuming that at each frequency corresponds a unique wave vector ($\mathbf{k} \cdot \delta\mathbf{B} = 0$), shows that these short time emissions have a right-hand circular polarization and parallel wave vector (not shown). However, only a k-filtering analysis such as the one carried out by [33] in the magnetosheath region will fully determine the wave vector of these intense waves and will permit to estimate a possible Doppler shift effect. Indeed, assuming a plasma velocity of 1000 km/s with a wavelength of $c/\omega_{pe} \simeq 10$ km gives a Doppler shift about 100 Hz. Now, we focus on one of the most intense short duration emission observed between 1657:00 and 1657:30 UT. We can see on Fig. 5 panels 2 and 4 that Cluster detects a current structure with a spatial scale comparable to or smaller than the intersatellite distance of 200 km, as B_y and B amplitudes are strongly different on C4 than on the others s/c. Therefore this current structure has a scale smaller than the proton Larmor radius or proton inertial length which are about 1000 km. Associated with this small scale current structure and minimum of the modulus of **B**, we observe on C2 (red) an electromagnetic wavepacket with a huge magnetic amplitude of ± 1 nT whereas the electric field amplitude is about ± 2 mV/m (panels 5 and 6). Note that this wavepacket is also detected on C1 and C3 (not shown) but not on C4 (blue). Therefore the wavepacket seems to be very localized within the current structure. Furthermore one can remark that intense quasi-electrostatic structures are detected before

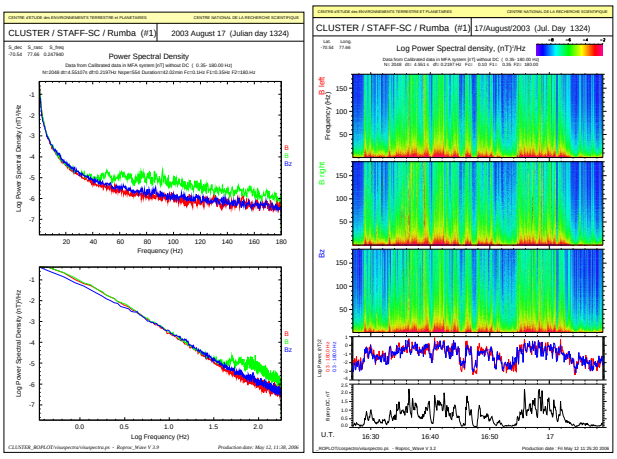

Fig. 4. Fourier spectra (left picture) and spectrograms (right picture) of magnetic fluctuations from STAFF-SC data in a MFA frame (δB_z corresponding to $\delta B_{\parallel}$). The time resolution of the spectrogram is 4.55 s and the frequency resolution is 0.22 Hz. The lower cut-off frequency has been fixed at 0.35 Hz to get rid of any spin modulation effect (see text for more details).

and after this electromagnetic wavepacket. On panels 7 and 8, electron and ion moments are plotted but clearly the magnetic field varies strongly on the 4 s time resolution of particle measurements. Thus there is a large uncertainty in the calculation of particle moments ($V_{xi} \simeq 1000$ km/s and $V_{yi} \simeq -500$ km/s, $V_{xe} \simeq \pm 2000$ km/s and $V_{ye} \simeq 2000$ km/s). These moments can also fluctuate over a time scale shorther than 4 s. For the same reasons, the comparison between the current density, computed from curlB, and from particles (panels 9 and 10) can just be done qualitatively. One can remark that during most of the time interval the ion current density (thick blue line) is directed antiparallel to curlB, which implies that the electron should be the current carriers in the s/c frame. In average the trend of the electron currents (J_x and J_y) agree quite well with curlB calculations. Finally, the current density measurements (from curlB) show that the magnetic wave packet is associated with intense currents up to 60 nA/m^2 (J_x) and to 80 nA/m^2 (J_z not shown). These intense currents seem to be parallel as well as perpendicular to the magnetic field (pink dotted line). Therefore a modeling of these intense whistler waves requires a stability analysis of a three-dimensional CS equilibrium. Finally, the high-time resolution electron fluxes show a strong anisotropy and enhanced fluxes (first and second panels from the bottom) in association with the large amplitude magnetic field fluctuations, while Cluster is still located in the plasma sheet. At this stage, we speculate that this anistropy corresponds to larger fluxes parallel to $\mathbf{B}$ than perpendicular. Fluxes as a function of electron pitch angle will be showed in a next paper in order to confirm this point. Nevertheless, these observations are sufficient to indicate that the electron dynamics seems to be strongly related to the whistler wave activity, as expected in the electron MHD regime.

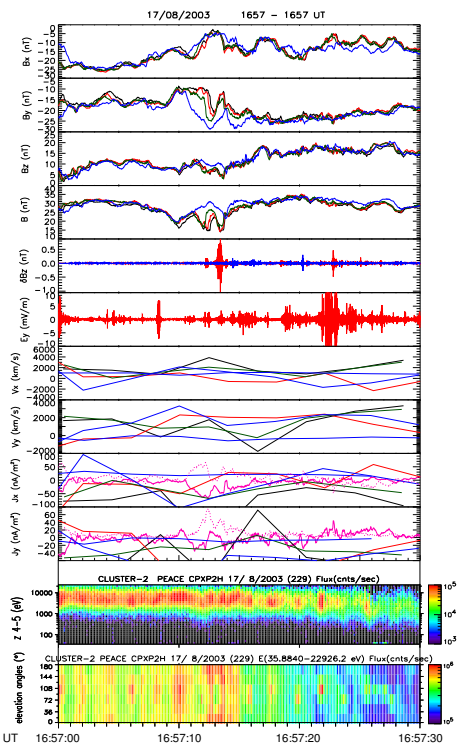

Fig. 5. All data are plotted in GSM coordinates excepted the electric and magnetic field fluctuations in SR2 frame: B_x, B_y, B_z, B components of the magnetic field, δB_z, δE_y components of the electric and magnetic fields from 30 Hz to 180 Hz, V_x and V_y components of electron (thin colored line) and ion (thick colored line) velocities, J_x and J_y components of the electrical current density computed from curlB (pink line) and from electron (thin colored line) and ion (thick colored line) moments. The pink dotted line in J_x panel corresponds to the parallel current density while the pink dotted line in J_y panel corresponds to the perpendicular current. Two last panels are the high-time resolution (125 ms) electron fluxes: (i) for different energy ranges (from 35.8 eV - 22.9 keV) for one angular sector and (ii) integrated in energy for different angular sectors respectively.

3. Discussion

In addition to low-frequency ballooning modes which are regularly observed during substorm expansion phase [31, 10, 37, 18], as well as on present data, we have shown that intense waves ($f \simeq f_{H+} \simeq f_{be} \simeq 0.2$ Hz) are detected together with a fast thickening of the CS. The association of these waves with dipolarisation and fast flows was reported also all through the tail [27, 36, 26, 37]. It was suggested by [16] that the level of emission of the waves may control the plasma transport in the magnetotail and that this mechanism can be efficient all through the tail using GEOS-2, Geotail and Cluster data [17]. It was shown by [25] that the waves can be generated by a parallel current instability as soon as the drift velocity between protons and electrons is close to the proton thermal velocity. However, the fact that the proton cyclotron frequency is very close to the electron bounce frequency implies that any consistent theoretical calculations should take into account the effect of the bounce motion of electrons on the

growth rate of the instability. Such a study considering the parallel current driven instability is currently on progress. Furthermore, while classical wave polarization analysis fail to characterize these waves, we have shown, using the current density measurements, that these waves corresponds to intense parallel current density fluctuations and perpendicular magnetic field fluctuations. These results should be taken into account in the future as constraints for testing any instabilities as a source of these emissions. At smaller scale and higher frequencies, we have identified intense short duration (< 4 s) whistler emissions ($f < f_{ce} \simeq 400$ Hz for $B_0 = 15$ nT) during the oscillations of the thin current sheet.The classical dispersion relation of whistler (helicon) waves [13], assuming $\omega \ll \omega_{ce}$ gives: $\omega/(k_\parallel v_A) = (\omega/\omega_{ci})^{1/2} \simeq 14$ at $f = 40$ Hz and agrees with the phase velocity obtained from the ratio of $\delta E(\omega)/\delta B(\omega) \simeq 20000$ km/s. These intense whistler waves are observed in association with small scale ($l \simeq$200 km $< \rho_i \simeq c/\omega_{pi}$) current structures. These kind of waves belongs to the regime of electron magnetohydrodynamics described theoretically by [5, 15]. It was shown in a laboratory experiment by [40] that a pulse of current at the whistler time scale propagates through the plasma by a whistler waves and suggest by analogy to "Alfvén wing" to speak about "whistler wing". Therefore two different questions can be adressed for understanding the existence of such intense whistler waves: (1) what is the origin of such small scale current structures with $c/\omega_{pe} < l < c/\omega_{pi}$?(2) what produces such pulses of current at the whistler time scale? In the former case we can suggest that proton cyclotron/electron bounce waves may generate such small scale current structures which can in turn generate whistler waves. In the latter case, we suggest that the short duration pulse of current could be generated by a fast reconnection process as described by [5, 2]. To summarize we can distinguish two scenarii (1) top/bottom: at the scale of the current sheet, the CS eigen modes correspond to low-frequency waves like ballooning. The parallel and perpendicular current fluctuations associated with ballooning modes can cause parallel [25] or perpendicular [21] current driven instablities at $\omega \simeq \omega_{ci}, \omega_{be}$. Then these instabilities create small scale current structure which can generate intense whistler waves. On the other hand a bottom/top scenario corresponding to an inverse cascade, as suggested by [20]. However, in the present case the process would start by a fast reconnection at $\omega_{ci} < \omega < \omega_{ce}$ and at small scale $c/\omega_{pe} < l < c/\omega_{pi}$. The corresponding fluctuations could provide a kind of anomalous resistivity for lower frequency instabilities with larger spatial scale. Note that the whistler waves are also expected by collisionless magnetic reconnection models in the ion diffusion region ($\leq c/\omega_{pi}$). However, hybrid simulation results showed the formation of a standing whistler wave close to the separatrix (e.g. [35]). Given our observations of numerous short-duration emissions of whistler wave in association with small scale current structure, Cluster would have to remain close to the separatrix during the whole period which seems unlikely. Finally, the full characterization of such small scale structures will not be possible due to the time resolution of the particle measurement. Furthermore, even smaller scale structures c/ω_{pe}, the so-called "electron diffusion region" are already detected in the subsolar region [23] and are also expected in the magnetotail. Such studies are the principal objectives of the future Magnetospheric Multi-Scale (MMS) mission that includes optimized high-time resolution of particles as well as field measurements, three-dimensional electric field and small inter-satellite distances. On the other hand, the spatial distribution of such small scale structures and their role on the global dynamics of the magnetosphere will be adressed by the Time History of Event and Macroscale Interactions during Substorms (THEMIS) mission.

4. Conclusion

We have presented a substorm event and have shown that the pre-existing thin current sheet with a thickness of the order of the proton Larmor radius and current carried by electron (in the s/c frame) thickens under the effect of electromagnetic fluctuations at three scales. While the low-frequency ($\simeq 20$ mHz) scale has not been discussed in detail, we have shown that fluctuations at the proton cyclotron / electron bounce frequency ($0.2 - 10$ Hz) correspond to signatures of parallel current density fluctuations. They are detected in association with a fast thickening of the CS and accelerated particles suggesting a micro-instability as a source of these fluctuations as well as a trigger for the CS thickening, and the subsequent fast flow. At higher frequencies, we have identified short duration bursts ($<$ 4 s) of whistler waves (right-hand circular polarization with $\mathbf{k} \cdot \mathbf{B_0} \simeq 0$) associated with small scale current structures ($l < \rho_i \simeq c/\omega_{pi}$) during the whole substorm period. Focussing on a particularly intense burst of whistler waves we have shown that these bursts are also associated with enhanced electron fluxes with a strong anisotropy. More investigations are needed to understand the origin of these whistler waves and their coupling with the other scales.

References

1. Asano, Y., Mukai, T., Hoshino, M., Saito, Y., Hayakawa, H., and Nagai, T., Current sheet structure around the near-earth neutral line observed by geotail, *J. Geophys. Res.*, 109, doi: 10.1029/2003JA010114, 2004.
2. Attico, N., Califano, F., and Pegoraro, F., Kinetic regimes of high frequency magnetic reconnection in a neutral sheet configuration, *Phys. Plasmas*, 9, 458–464, 2002.
3. Balogh, A., *et al.*, The Cluster magnetic field investigation, *Space Science Reviews*, 79, 65–91, 1997.
4. Biskamp, D., Schwarz, E., and Drake, J. F., Two-fluid theory of collisionless magnetic reconnection, *Phys. Plasmas*, 4(4), 1002–1009, 1997.
5. Bulanov, S. V., Pegoraro, F., and Sakharov, A. S., Magnetic reconnection in electron dynamics, *Phys. Fluids B*, 4, 2499–2508, 1992.
6. Cheng, C. Z. and Lui, A. T. Y., Kinetic ballooning instability for substorm onset and current disruption observed by AMPTE/CCE, *Geophys. Res. Lett.*, 25, 4091, 1998.
7. Cornilleau-Wehrlin, N., *et al.*, The CLUSTER spatio-temporal analysis of field fluctuations (STAFF) experiment, *Space Science Reviews*, 79, 107–136, 1997.
8. Daughton, W., Nonlinear dynamics of thin current sheets, *Phys. Plasmas*, 9(9), 3668–3678, 2002.
9. Daughton, W., Electromagnetic properties of the lower-hybrid drift instability in a thin current sheet, *Phys. Plasmas*, 10(8), 3103–3119, 2003.

10. Erickson, G. M., Maynard, N. C., Burke, W. J., Wilson, G. R., and Heinemann, M. A., Electromagnetics of substorm onsets in the near-geosynchronous plasma sheet, *J. Geophys. Res.*, 105, 25265–25290, 2000.
11. Gustafsson, G., *et al.*, The electric field and wave experiment for the cluster mission, *Space Science Reviews*, 79, 137, 1997.
12. Harris, E. G., On a plasma sheath separating regions of oppositely directed magnetic field, *Il Nuovo Cimento*, XXIII, 115, 1962.
13. Heliwell, R. A., *Whistlers and Related Ionospheric Phenomena*, Standfor University Press, Standford, CA, 1965.
14. Johnstone, A., *et al.*, PEACE: A plasma electron and current experiment, *Space Science Reviews*, 79, 351–398, 1997.
15. Kingsep, A. S., Chukbar, K. V., and Yankov, V. V., Electron magnetohydrodynamics, *in Reviews of Plasma Physics*, volume 16, edited by B. Kadomtsev, 243, Consultants Bureau, New York, 1990.
16. Le Contel, O., Roux, A., Perraut, S., Pellat, R., Holter, Ø., Pedersen, A., and Korth, A., Possible control of plasma transport in the near-earth plasma sheet via current-driven Alfvén waves ($f \simeq f_{H+}$) during substorm growth phase and relation to breakup, *J. Geophys. Res.*, 106, 10817–10827, 2001.
17. Le Contel, O., *et al.*, Role of the parallel current instability during substorms: Theory and observations, *in Sixth International Conference on Substorms(ICS-6), March 25-29, 2002*, edited by R. Winglee, 326–333, University of Washington, Seattle, 2002.
18. Louarn, P., Fruit, G., Budnik, E., Sauvaud, J.-A., Jacquey, C., Lucek, E., the CDPP, CIS, and teams, F., Low frequency fluctuations of the plasma sheet - cluster observations and models, *in Eighth International Conference on Substorms (ICS-8), March 27-31, 2006*, edited by E. Donovan, University of Calgary, Canada, 2006, this issue.
19. Lui, A. T. Y., Current controversies in magnetospheric physics, *Rev. Geophys.*, 39(4), 535–563, 2001.
20. Lui, A. T. Y., Relating plasma instabilities in the magnetotail to observables, *in Eighth International Conference on Substorms (ICS-8), March 27-31, 2006*, edited by E. Donovan, University of Calgary, Canada, 2006, this issue.
21. Lui, A. T. Y., Chang, C.-L., Mankofsky, A., Wong, H.-K., and Winske, D., A cross-field current instability for substorm expansions, *J. Geophys. Res.*, 96, 11389–11401, 1991.
22. Mandt, M. E., Denton, R. E., and Drake, J. F., Transition to whistler mediated magnetic reconnection, *Geophys. Res. Lett.*, 21(1), 73–77, 1994.
23. Mozer, F. S., Bale, S. B., McFadden, J. P., and Torbert, R. B., New features of electron diffusion regions observed at subsolar magnetic field reconnection sites, *Geophys. Res. Lett.*, 32, L24102, doi:10.1029/2005GL024092, 2005.
24. Perraut, S., Le Contel, O., Roux, A., Parks, G., Hoshino, M., Mukai, T., and Nagai, T., Substorm expansion phase: Observations from Geotail, Polar and IMAGE network, *J. Geophys. Res.*, 108, 1159, doi:10.1029/2002JA009376, 2003.
25. Perraut, S., Le Contel, O., Roux, A., and Pedersen, A., Current-driven electromagnetic ion cyclotron instability at substorm onset, *J. Geophys. Res.*, 105, 21097–21107, 2000.
26. Perraut, S., Le Contel, O., Roux, A., Pellat, R., Korth, A., Holter, Ø., and Pedersen, A., Disruption of parallel current at substorm breakup, *Geophys. Res. Lett.*, 4041–4044, 2000.
27. Perraut, S., Morane, A., Roux, A., Pedersen, A., Schmidt, R., Korth, A., Kremser, G., Aparicio, B., and Pellinen, R., Characterization of small scale turbulence observed at substorm onsets: Relationship with parallel acceleration of particles, *Adv. Space Res.*, 13(4), 217, 1993.
28. Rème, H., *et al.*, The CLUSTER Ion Spectrometry Experiment, *Space Science Reviews*, 79, 303, 1997.
29. Robert, P., Dunlop, M., Roux, A., and Chanteur, G., Accuracy of current density determination, *in Analysis Methods for Multi-Spacecraft Data*, edited by G. Paschman and P. Daly, ISSI Scientific Report SR-001, chapter 16, 395–418, European Space Agency, 1998.
30. Roux, A., Le Contel, O., Fontaine, D., Louarn, P., Sauvaud, J.-A., and Fazakerley, A. N., Role of instabilities at substorms, *in Eighth International Conference on Substorms (ICS-8), March 27-31, 2006*, edited by E. Donovan, University of Calgary, Canada, 2006, this issue.
31. Roux, A., Perraut, S., Robert, P., Morane, A., Pedersen, A., Korth, A., Kremser, G., Aparicio, B., Rodgers, D., and Pellinen, R., Plasma sheet instability related to the westward traveling surge, *J. Geophys. Res.*, 96, 17697, 1991.
32. Runov, A., *et al.*, Current sheet structure near magnetic x-line observed by cluster, *Geophys. Res. Lett.*, 30(11), 1579, doi: 10.1029/2002GL016730, 2003.
33. Sahraoui, F., *et al.*, Ulf wave identification in the magnetosheath: the k-filtering technique applied to cluster II data, *J. Geophys. Res.*, 108, 1335, doi:10.1029/2002JA009587, 2003.
34. Schindler, K. and Birn, J., Models of two-dimensional embedded thin current sheets from Vlasov theory, *J. Geophys. Res.*, 107, 1193, doi:10.1029/2001JA000304, 2002.
35. Shay, M. A., Drake, J. F., Denton, R. E., and Biskamp, D., Structure of the dissipation region during collisionless magnetic reconnection, *J. Geophys. Res.*, 103, 9165–9176, 1998.
36. Shinohara, I., Nagai, T., Fujimoto, M., Terasawa, T., Mikai, T., Tsuruda, K., and Yamamoto, T., Low-frequency electromagnetic turbulence observed near the substorm onset site, *J. Geophys. Res.*, 103, 20365, 1998.
37. Sigsbee, K., Cattell, C. A., Fairfield, D., Tsuruda, K., and Kokubun, S., Geotail observations of low-frequency waves and high-speed earthward flows during substorm onsets in the near magnetotail from 10 to 13 R_E, *J. Geophys. Res.*, 107, 1141, doi: 10.1029/2001JA000166, 2002.
38. Sitnov, M. I., Malova, H. V., and Sharma, A. S., Role of the temperature ratio in the linear stability of the quasi-neutral sheet tearing mode, *Geophys. Res. Lett.*, 25, 269–272, 1998.
39. Tikhonchuk, V. T. and Rankin, R., Electron kinetic effects in standing shear alfvén waves in the dipolar magnetosphere, *Phys. Plasmas*, 7(6), 2630–2645, 2000.
40. Urrutia, J. M. and Stenzel, R. L., Transport of current by whistler waves, *Phys. Rev. Lett.*, 62(3), 272–275, 1989.
41. Wilber, M., *et al.*, Cluster observations of velocity space-restricted ion distributions near the plasma sheet, *Geophys. Res. Lett.*, 31, L24802, doi:10.1029/2004GL020265, 2004.